COHERENT AND INCOHERENT TUNE SHIFTS DEDUCED FROM IMPEDANCE MODELLING IN THE ESRF-RING

T.F.Günzel, ESRF, Grenoble, France

Abstract

In single bunch the detuning of the transverse modes m=0,1 and –1 is calculated on the base of an impedance model built up from element-wise wakefield calculation and the resistive wall impedance of the ESRF-ring. As the vacuum chambers of the ESRF storage ring have notably flat cross sections, incoherent wake fields have an important impact on the tune shifts as well as coherent wake fields. Compared to tune shifts measurements in single bunch the calculated transverse mode detuning can explain half the tune shift in the vertical plane and almost completely the tune shift in the horizontal plane.

INTRODUCTION

The operation of the ESRF-ring in single bunch is strongly affected by low current thresholds of the Transverse Mode Coupling Instability. Several impedance models were proposed for the vertical plane[1,2], however, for the horizontal plane an impedance model has not been developed as yet. In this paper a model is proposed which fits quite well with the measured tune shifts of single bunch in both planes because it distinguishes between tune shifts from coherent and incoherent wake fields. It turns out that the asymmetric cross section of the vacuum chambers, essentially that of the low-gap sections, gives rise to an important incoherent tune shift component to the total tune shift. R.Nagaoka has already recognised that the incoherent tune shift plays a major role in the transverse mode detuning[3].

DECOMPOSITION OF THE WAKEFIELD

For the calculation of the wakefields of geometrical origin GdfidL[4] was used. Details are described in [2]. Several authors[5,6] have already pointed out that, in asymmetric chambers, resistive wall wakes have a component which is quadrupolar and only depends on the witness particle position. This component was also searched for with GdfidL in wakes created only by a geometry variation. Indeed for the standard ESRF-vacuum chamber and the low-gap chambers (fig.1) the wakes can be decomposed into a dipolar component, which depends only on the position of the exciting particle, and a component which is quadrupolar depending only on the position of the witness particle. Therefore a transverse wake calculated with a small transverse offset of the exciting particle has first to be decomposed into its coherent part and its incoherent part. Only the coherent wake is used for the impedance calculation. This procedure, henceforth referred to as "detuning wake correction", reduces the amplitude of the original vertical wake and increases the amplitude of the horizontal wake at the bunch position by about the same amount. In fact only this correction makes the horizontal impedance calculation possible. The incoherent wake has to be treated seperately and, as it depends only on the position of the witness particle, gives rise to an incoherent tune shift. However, in an axial symmetric geometry (for instance the cavities) the incoherent wake does not occur. Furthermore it was found that, in a vertical flat chamber cross section, a vertical geometry variation creates large dipolar and quadrupolar wakes, whereas a horizontal geometry variation has almost no effect. Consequently the horizontal impedance is mainly of vertical origin while horizontal variations in the vacuum chamber do not play a significant role.

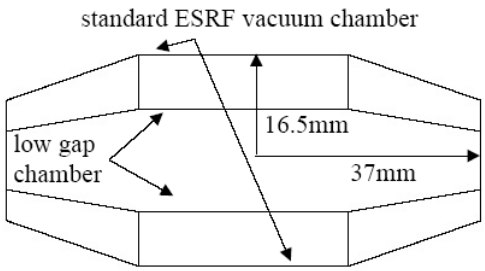

figure 1: overlay of the standard vacuum chamber cross section with a low gap chamber cross section (schematic)

RESISTIVE WALL IMPEDANCE

For the resistive wall impedance budget the same wake field decompostion is applied. According to this decomposition[6] for flat chamber cross sections the vertical $Z^V(\omega)$ and horizontal impedance $Z^H(\omega)$ only depend on one parameter, the vertical half-extension of the chamber ***a*** (single wall material infinitely extended):

$$Z^V(\omega) = 2 \cdot Z^H(\omega) = \frac{\pi^2}{12}(1+i)\frac{Z_0}{2\pi a^3}\delta(\omega)$$

with Z_0=376,73Ω and $\delta(\omega)$ as skin depth of the chamber wall material. Even if the chamber is not completely flat, this remains a good appoximation [6]. In case of a NEG-coated vacuum chamber the wall is considered as a double layer which changes the $\omega^{-0.5}$ behaviour of the skin depth[7]. Investigations of the impedance of NEG-coated vacuum chambers are still ongoing. Hence in order to adopt a simplified modelisation the $\omega^{-0.5}$ behaviour was maintained but scaled to provide the kick factor of a double layer (NEG/Cu or NEG/Al). Furthermore, each contribution is weighted by the local β-function of the corresponding element. The total horizontal weighted impedance is larger than the vertical one. Two thirds of the vertical weighted impedance is

table 1: Resistive wall impedance budget: the two last columns indicate (in units of $(1+i)M\Omega\sqrt{GHz/\omega}$ with ω as the angular frequency) the vertical and horizontal weighted resistive wall impedance assuming a flat cross section. Different chamber types were integrated in one line, which explains the fractional figures of quantity. β_V and β_H are the vertical and horizontal β-functions.

chamber type\material\length	half-gap [mm]	quantity	β_V [m]	β_H [m]	$Z_V\beta_V$	$Z_H\beta_H$
ESRF standard chamber\stainless steel \672m	16.5	1	24.6	16.6	6.22	2.10
low-gap chamber\ stainless steel or AL/NEG \ 5m	5.5	13.26	3.4	23.7	2.34	8.13
low-gap chamber\ stainless steel/Cu/NEG or Al/NEG \ 5m	4	6.28	3.5	24.9	0.76	2.73
invacuum and minigap(open)\Cu or stainless steel\1m/1.6m/2m	15	8.13	3.7	23.8	0.01	0.01
remaining elements					0.52	0.88
		TOTAL			**9.86**	**13.85**

made up of the standard ESRF vacuum chamber, whereas the low-gap chambers dominate in the horizontal impedance budget. The reason for this are the β-functions whose mean values are 19.9m horizontally and 3.42m vertically inside a straight section with a low-gap chamber, whereas in the remaining part of the ring, the vertical value (24.9m) is larger than the horizontal one (16.8m) (table 1).

GEOMETRICAL IMPEDANCE

In order to establish the geometrical impedance budget the wakes of a large number of elements (taper pairs, invacuum undulators, RF-fingers, flanges, horizontal pumps, the cavities and their tapers, scrapers, BPM's, the kicker chambers and the septum) of the storage ring were calculated with GdfidL. The detuning wake correction and the weighting with the local β-functions were applied for the calculation of vertical and horizontal impedance (fig.2). RF-fingers and flanges dominate in the vertical impedance budget, whereas in the horizontal impedance budget, the low-gap chambers dominate. A superposition of 4 broadband resonators (4 BBR) was fitted to the obtained spectra. Combined with the transverse resistive wall impedance the obtained fit

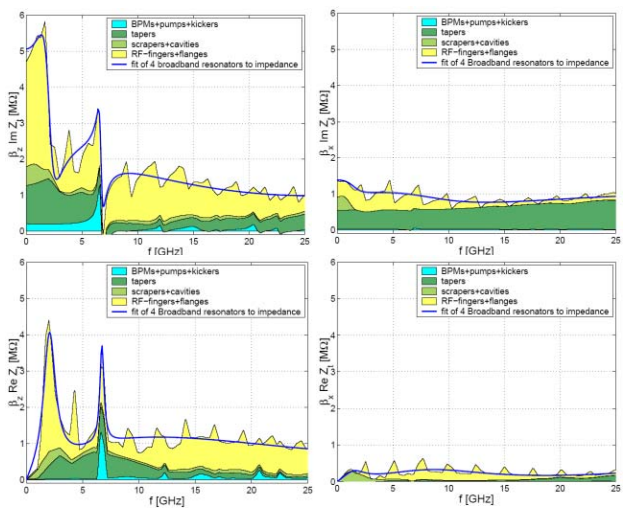

figure 2: Geometrical impedance budget, vertical(left) and horizontal(right). The blue curve is the 4 BBR-fit

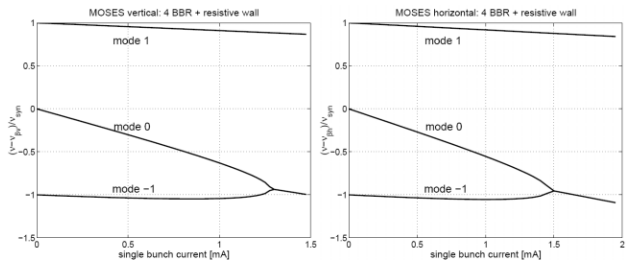

figure 3: vertical (left) and horizontal (right) mode detuning from the 4BBR and resistive wall impedance

parameters were entered into MOSES (modified to also accept resistive wall impedance)[8]. The predicted coupling between mode 0 and –1 in the vertical plane is attained at 1.25mA, and at 1.5mA in the horizontal plane (fig.3).

THE INCOHERENT TUNE SHIFTS

The incoherent tune shift per current dν/dI was calculated by adding the quadrupolar wakes by using:

$$\frac{d\nu}{dI} = \frac{1}{2\,\omega_0\,(E/e)} \sum_i \beta_i \kappa_i$$

where ω_0 is the angular revolution frequency, E the beam energy, e the electron charge, β_i the β-functions and κ_i the transverse kick factors of the contributing machine elements. The transverse kick factors were calculated in time domain from the quadrupolar wakes of geometric origin (fig.4) and in frequency domain from the "incoherent part of the resistive wall impedance"

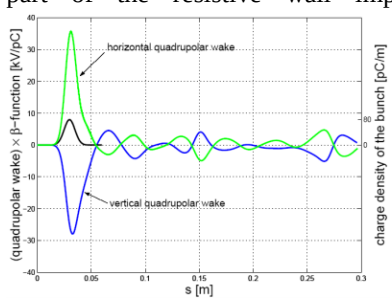

figure 4: the total incoherent quadrupolar geometrical wakes and the bunch profile for the kick factor calculation

(according to [6] $Z^V(\omega)/2$ vertical and $-Z^H(\omega)$ horizontal). The assumed bunch length was 5mm.

The formula above was also used to calculate the coherent tune shifts caused by the dipolar coherent wakes to compare their values to the incoherent ones. For this comparison only the kick factor sum weighted by the β-function was evaluated (fig.5). The results show that the incoherent horizontal tune shift is opposite to the coherent one which leads to a compensation of both. On the other hand the coherent and incoherent vertical tune shift add up positively. The geometric and resistive wall impedance contribute almost equally to the total vertical kick factor sum, whereas the resistive wall impedance contributes twice more to the total horizontal kick factor than the geometrical impedance.

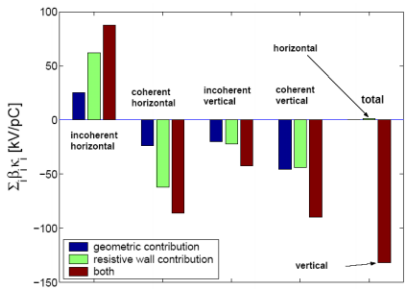

figure 5: the different contributions to total vertical and horizontal kick factors (coherent and incoherent)

RESULTS

Finally the incoherent tune shifts were added to the coherent mode detuning. This only changes the slopes of the mode detuning, but not the current thresholds. The results are compared to measured data taken at RF-voltage of 8MV (fig.6). By normalization of all data on

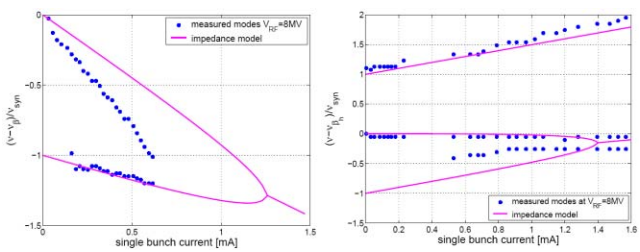

figure 6: measured and calculated mode detuning against single bunch current in the vertical (left) and horizontal plane (right). ν_{SYN} denotes the synchrotron tune

the synchrotron tune only the effective impedances of the different modes are bunchlength (respectively RF-voltage) dependent. In the vertical plane the model can explain about half of the mode 0 detuning. As a consequence the current threshold is higher (1.3mA compared to measured 0.65mA). However, the detuning of mode –1 is quite well reproduced. In the horizontal plane the indifference of mode 0 to the current is due to the compensation of the coherent and incoherent tune shifts, furthermore the slope of mode 1 is well reproduced. The measured data of mode –1 is less accurate due to the difficult recognition of the mode at nearly zero chromaticity. Consequently the reproduction is also less convincing. However, the calculated threshold of 1.5mA is quite close to that measured at 1.3mA. The model also reproduces data taken at different RF-voltages.

CONCLUSION

Wakefields created in non-axial geometries can be decomposed into a dipolar coherent part which depends on the position of the exciting particle and a quadrupolar incoherent part, which depends only on the witness particle. This was found in wakes of geometrical and resistive wall nature. Consequently, for a vertically flat chamber, transverse impedances are essentially created by vertical (geometry variation and resistive wall) effects. The vertical impedance (both types) of the ESRF-machine is created by machine elements of different types, whereas the horizontal impedance (both types) is mainly determined by the low-gap chambers. The β-function distribution along the ring is mainly responsible for that. The vertical impedance budget can explain half of the measured vertical tune shift, the horizontal one is fully reproduced. The notable detuning of the vertical mode -1 can be explained by the incoherent vertical tune shift, a broadband model with a high cut-off frequency is not necessary.

Future tasks are notably to look for the remaining vertical impedance. The results may also have important consequences for the design of vacuum chambers in future storage rings.

ACKNOWLEDGEMENTS

The author thanks R.Nagaoka for fruitful discussions on incoherent and coherent tune shifts and JL Revol for his feedback and good support concerning measurements.

REFERENCES

[1] R.Nagaoka, JL Revol, P.Kernel, G.Besnier, Trans. Instabilities in the ESRF Storage Ring, PAC 1999

[2] T.F.Günzel, Evaluation of the vertical trans. Impedance of the ESRF-machine by element-wise wakefield calculation, EPAC 2002

[3] R.Nagaoka, Impact of resistive-wall wake fields generated by low-gap chambers on the beam at the ESRF, EPAC 2002

[4] W.Bruns, GdfidL - a Finite Difference Program with Reduced Memory and CPU Usage, PAC 1997

[5] R.L. Gluckstern, J. van Zeijts, B. Zotter, Coupling Impedance of beam pipes of general cross section, Physical Review **E47 (**1993), 656

[6] K.Yokoya, Resistive Impedance of Beam Pipes of General Cross Section, Part. Acc. **41(**1993**),** 221

[7] A.Burov, V.Lebedev, Transverse resistive wall impedance of a multi-layer round chamber, EPAC 2002

[8] Y.H.Chin, MOSES, CERN/LEP-TH/88-5